Catalysis
Science & Technology

RSCPublishing

PAPER

View Article Online
View Journal | View Issue

Published on 19 July 2013. Downloaded by State University of New York at Stony Brook on 30/10/2014 15:17:32.

Cite this: *Catal. Sci. Technol.*, 2013, **3**, 2993

Magnetically recoverable AuPd nanoparticles prepared by a coordination capture method as a reusable catalyst for green oxidation of benzyl alcohol†

Tiago A. G. Silva,[a] Richard Landers[b] and Liane M. Rossi*[a]

Received 16th April 2013,
Accepted 26th June 2013

DOI: 10.1039/c3cy00261f

www.rsc.org/catalysis

AuPd nanoparticles (AuPd NPs) have received considerable attention because of their importance as catalysts in selective aerobic oxidations; however, improved synthetic methods for making them reusable catalysts are necessary. Here, we present the preparation of magnetically recoverable AuPd NPs by immobilizing pre-synthesized PVA-stabilized AuPd NPs onto magnetic supports. The immobilization method is based on the functionalization of the support with strong coordinating ligands, such as amino and thiol, for the attachment of AuPd NPs containing weak coordinating groups. We were able to increase the metal loading by a coordination capture method with functionalized supports, but the ligands grafted on the support surface affected the catalytic activity of AuPd NPs. Moreover, the amino groups provided stabilization in solution, which made the catalyst separation after reaction difficult. Finally, we obtained highly active and recyclable catalysts by removing the functional groups by a thermal treatment. Negligible metal leaching and catalyst recycling in successive reactions are important features of the new catalytic system.

Introduction

Aldehydes are valuable chemicals both as very active intermediates in organic synthesis and as high value components for the perfume industry. They can be prepared by the oxidation of primary alcohols, an important laboratory and commercial procedure,[1,2] traditionally performed using stoichiometric oxidants that are major sources of toxic wastes in organic synthesis. Replacement of stoichiometric oxidation methods by heterogeneously catalyzed selective aerobic oxidation methods prompted the need for the development of more efficient solid catalysts.[3] In recent years, the unexpectedly high activity and selectivity of Au nanoparticle (Au NP) catalysts in different reactions, for example oxidation reactions, have stimulated intensive research into the use of Au NPs.[4] In contrast, there are few examples of gold-catalysed homogeneous oxidation reactions.[5] Rossi and Prati and co-workers[6–8] were the first to demonstrate that alcohols, in particular diols and sugars, can be oxidized by Au NP catalysts to give various monoacids, as long as a base is present. Aerobic oxidation and oxidative esterification of benzyl alcohol are model reactions catalyzed by supported Au NPs that also resulted in higher conversions to benzaldehyde and esters in the presence of a base. The requirement for a strongly alkaline medium for the oxidation reaction to occur at acceptable rates may represent a considerable limitation to the use of Au NP catalysts, as side reactions can lower the catalyst selectivity (keto–enol equilibration, Cannizzaro reaction, oxidative decarbonylation), or the catalyst/catalyst support can be attacked in basic media.[9,10] We recently prepared Au NPs supported on a silica-coated magnetic support, which exhibited clean, fast and efficient separation after chemical reactions by means of the application of an external magnetic field.[11] The catalyst was highly active in the oxidation of alcohols and could be successfully separated from the reaction products; however, the Au NPs suffered the consequences of the use of a base, such as support corrosion due to the action of the base, and the catalysts grew into larger (~80 nm) and less active or inactive particles. The initially very active catalyst lost activity gradually when used in successive reactions.

In order to avoid the problems mentioned above caused by the use of a base, we chose to adhere to the literature that says that the combination of Au with a second metal from the platinum group can avoid the use of a base and still give high conversion and selectivity in the oxidation of alcohols. A bimetallic catalyst, *i.e.* 1% Au–0.1% Pd/Al_2O_3, was used for the transformation of 6-hydroxyhexanoic acid to adipic acid in the absence of a base.[12] Hutchings and co-workers[13] have shown that the alloying of gold with palladium leads to a twenty-five-fold enhancement in activity in the oxidation of

---

[a] *Departamento de Química Fundamental, Instituto de Química, Universidade de São Paulo, Av. Prof. Lineu Prestes 748, São Paulo, 05508-000, SP, Brazil. E-mail: lrossi@iq.usp.br; Fax: +55 11 38155579*

[b] *Instituto de Física, UNICAMP, Campinas, 13083-970, SP, Brazil*

† Electronic supplementary information (ESI) available. See DOI: 10.1039/c3cy00261f

This journal is © The Royal Society of Chemistry 2013

Published on 19 July 2013. Downloaded by State University of New York at Stony Brook on 30/10/2014 15:17:32.

alcohols compared to monometallic catalysts with the simultaneous retention of selectivity. The oxidation of alcohols by AuPd NPs has received attention as an excellent alternative to the monometallic catalysts.[14–17]

In this paper we report the immobilization of pre-synthesized PVA-stabilized AuPd NPs on magnetically responsive materials. In order to explore the potential utilization of magnetic separation in the recovery of metal nanoparticles from their reaction mixture after liquid phase catalysis, the ability to attach them to the surfaces of a magnetic material is an important issue. Methods to immobilize nanoparticles on different surfaces are continuously being developed.[18] The metal nanoparticle–support linkage can occur on the basis of electrostatic interactions or covalent bonding. In both cases, nanoparticles and/or the support surface must be modified with complementary ligands to achieve the appropriate linkage between nanoparticles and the support. Ligands with various linkage capabilities can be readily introduced either on the surface of the support (for example, by means of organo-alkoxysilanes *in silica*) or into the metal NPs. Gold NPs can be well supported on silica by an electrostatic assembly of amino-modified silica spheres and citrate-coated Au NPs.[19] A modification of this method is based on the functionalization of the support with strong coordinating ligands and the impregnation of NPs synthesized with weak coordinating groups (for example, poly(vinyl-pyrrolidone) (PVP) or polyvinyl alcohol (PVA)), called the coordination capture method. The metal NPs are captured due to the affinity of ligands present in the functionalized support for the metal NPs. Khatri *et al.*[20] studied the deposition of ionic liquid-stabilized Au NPs on 3-mercaptopropyl-functionalized silica. The authors observed that the weakly coordinated ionic liquid molecules could be, to some extent, replaced with the thiol groups of the functionalized support. The Au–S chemisorption linkage resulted in strong immobilization of the Au NPs. This method can, in principle, be applied for the preparation of supported metal NPs for catalytic applications, but the effect of the functional groups grafted to the support on the catalytic performance has not been described.

Experimental

Synthesis of magnetite and silica-coated magnetite NPs

The synthesis of oleic acid-coated Fe_3O_4 NPs and the core–shell $Fe_3O_4@SiO_2$ composite has been reported elsewhere.[21] The solid was modified with amino groups by a reaction with 3-aminopropyltriethoxysilane (APTES) and with thiol groups by a reaction with 3-mercaptopropyltrimethoxysilane in dry toluene under N_2, to give the amino-functionalized ($Fe_3O_4@SiO_2$-NH_2) and thiol-functionalized ($Fe_3O_4@SiO_2$-SH) supports. The final solid was washed with toluene and dried at 100 °C for 20 h.

Synthesis of AuPd NPs

Gold–palladium NPs were synthesized as described by Hutchings and co-workers[22] by the reduction of 40 mL of a solution containing $HAuCl_4$ (16.5 μmol Au), $PdCl_2$ (16.5 μmol Pd) and polyvinyl alcohol (PVA) (6.0 mg) with 1.65 mL $NaBH_4$ (0.1 mol L^{-1}). The reaction was stirred for 30 min.

Synthesis of supported AuPd NPs

The catalyst support (500 mg) was added to 60 mL of water and the colloidal AuPd NPs solution prepared as above. The mixture was stirred at 25 °C for 2 h. The solid was then magnetically collected from the solution and washed with hot distilled water (2 × 25 mL) and ethanol (2 × 25 mL). The final solid was air-dried for 10 h. Samples of the prepared catalysts were calcined at 500 °C for 2 h.

Characterization

High-resolution transmission electron microscopy (HRTEM) was performed at the Brazilian Nanotechnology National Laboratory (LNNano, Campinas, SP) using a Jeol-3010 ARP microscope. Samples for TEM observations were prepared by placing a drop containing the nanoparticles on a carbon-coated copper grid. The histograms of the gold nanoparticle size distribution, assuming spherical shape, were obtained from the measurement of the diameters of about 300 particles found in arbitrarily chosen areas of enlarged micrographs. The samples were observed in different regions of the Cu grid.

The XPS spectra were obtained at the Instituto de Física (IF-UNICAMP) with a VSW HA-100 spherical analyzer using an aluminum anode (AlKα line, $h\nu = 1486.6$ eV) X-ray source. The high-resolution spectra were measured with a constant analyzer pass energy of 44 eV, which produces a FWHM line width of 1.7 eV for the Au 4f7/2 line. The powdered samples were pressed into pellets and fixed onto a stainless steel sample holder with a double-faced tape and analyzed without further preparation. To correct for charging effects, the spectra were shifted so that the Si 2p binding energy in SiO_2 was 103.5 eV. Curve fitting was performed by using Gaussian line shapes, and a Shirley-type background was subtracted from the data. The Pd/Au molar ratios were calculated using the Pd(3d5/2) and Au(4d5/2) XPS peak areas corrected using the corresponding Scofield cross-section values of 9.48 and 11.74, respectively.[23]

Catalytic experiments

The oxidation reactions were performed using a modified Fischer–Porter 100 mL glass reactor. In a typical solventless reaction, the glass reactor was loaded with the supported AuPd-catalyst (75 mg) and benzyl alcohol (9.6 mmol). The reactor, immersed in an oil bath, was loaded with O_2 to the desired pressure. The temperature was maintained by an oil bath placed on a hot stirring plate connected to a digital controller (ETS-D5 IKA). The reactions were conducted under magnetic stirring, using a Teflon-coated magnetic stir bar, for the desired time. The catalyst was magnetically recovered by placing a permanent magnet on the reactor wall. The products were collected using a syringe and analyzed by gas chromatography (GC) using *p*-xylene as the standard. The

This journal is © The Royal Society of Chemistry 2013

Published on 19 July 2013. Downloaded by State University of New York at Stony Brook on 30/10/2014 15:17:32.

isolated catalyst could be reused when a new amount of substrate was added.

Results and discussion

Catalyst preparation method and characterization

PVA-stabilized AuPd NPs were synthesized *via* $NaBH_4$ reduction of aqueous solutions containing a 1 : 1 molar ratio of Au(III) and Pd(II) metal salts in the presence of PVA. This polymer is known to bind weakly to metal nanoparticles, such that the reactants can access the nanoparticle surface in the presence of the stabilizer. Then, the AuPd NPs were immobilized on magnetically responsive supports, comprised of silica-coated magnetite NPs,[21] to give an additional property to the catalyst so that it can be easily recovered magnetically. This special support can be attracted to an external magnetic field; however, it will be able to carry the metal nanoparticles only if they are firmly attached to the support surface. In order to improve the catalyst–support interaction, the magnetic NPs were coated with a layer of silica and then functionalized with strong coordinating ligands, so the PVA-stabilized AuPd NPs were immobilized on the magnetically responsive material by a coordination capture method (Fig. 1). Silica was chosen because it is a very versatile support material, and displays some advantageous properties, such as easy functionalization of the surface silanol groups, which can react with various organo-trialkoxysilanes to attach organic groups to silica surface. The presence of such organic groups on the support surfaces has been shown to positively impact catalyst stability by improving metal–support interactions,[21] catalyst metal loading by impregnation,[24] and catalyst activity by tuning the size of metal NPs and their activity in hydrogenation reactions.[25] However, their influence on catalysts for selective aerobic oxidations has not been established.

Initially, an aqueous solution containing pre-synthesized AuPd NPs was added to non-functionalized and functionalized supports in order to evaluate the impregnation efficiency. After 2 h, the solids were isolated magnetically and the metal loading on the supports was measured by FAAS, as shown in Table 1. The non-functionalized support was loaded with 0.3 wt% AuPd, and the functionalized solids improved the uptake of the metal from the colloidal solution and allowed the preparation of catalysts with *ca.* 1 wt% AuPd.

Table 1 Metal loading in magnetically responsive supports

Support	Au (wt%)	Pd (wt%)	Au : Pd[a]	Au + Pd (mmol g^{-1})
Fe_3O_4	0.65	0.34	1 : 1	0.065
Fe_3O_4@SiO_2	0.20	0.10	~1 : 1	0.020
Fe_3O_4@SiO_2-NH_2	0.57	0.30	1 : 1	0.057
Fe_3O_4@SiO_2-SH	0.51	0.27	1 : 1	0.051

[a] Molar ratio.

The size and size distribution of the bimetallic AuPd NPs were assessed by the analysis of TEM micrographs such as those presented in Fig. 2. The TEM image of the Fe_3O_4@SiO_2-NH_2–AuPd NPs shown in Fig. 2A revealed the morphology of the catalyst support comprised of a core–shell nanostructure of magnetite coated with silica and AuPd NPs of 5.1 ± 1.2 nm in size decorating the support surface. The composition of the bimetallic NPs analyzed by FAAS revealed molar ratios close to 1 : 1 Au : Pd (Table 1); however it is not an easy task to discern whether AuPd NPs are random alloys or core–shell nanostructures. According to the methodology chosen for the solution synthesis of the bimetallic AuPd NPs, we can expect to obtain AuPd alloy NPs.[26] Analysis of the HRTEM micrographs of supported AuPd NPs, such as those presented in Fig. 2B, revealed a lattice spacing of 2.31 Å, which can be attributed to the AuPd(111) plane. This value is between the lattice spacing of Au(111) at 2.36 Å and Pd(111) at 2.23 Å. Monometallic planes were not found in the many NPs analyzed, suggesting that segregation of metals did not occur.

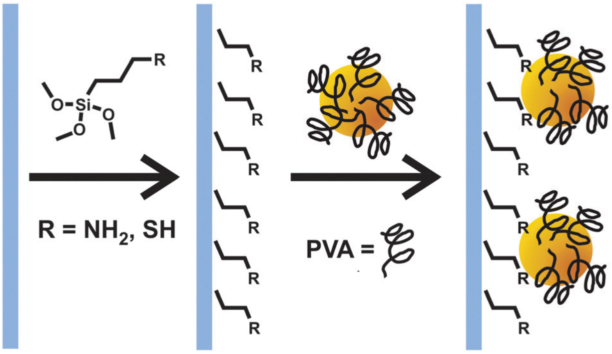

Fig. 1 Preparation of supported AuPd NP catalysts by a coordination capture method.

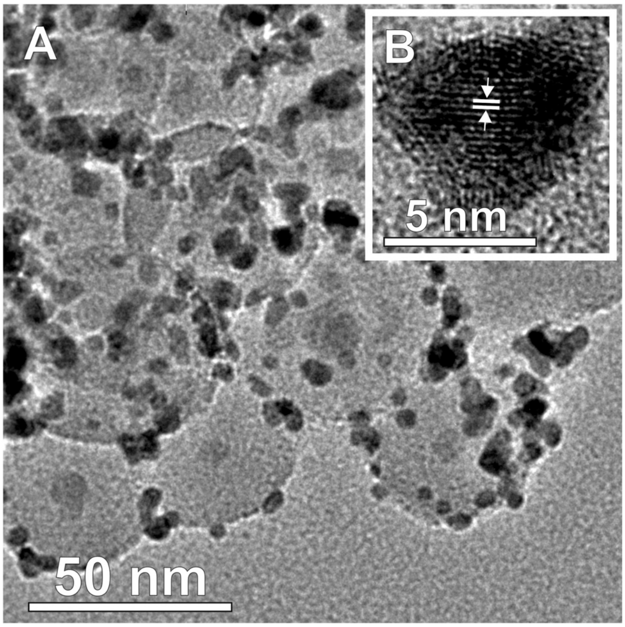

Fig. 2 (A) TEM image of AuPd NPs supported on Fe_3O_4@SiO_2-NH_2. (B) HRTEM micrograph of one AuPd NP with a lattice spacing of 2.31 Å.

Published on 19 July 2013. Downloaded by State University of New York at Stony Brook on 30/10/2014 15:17:32.

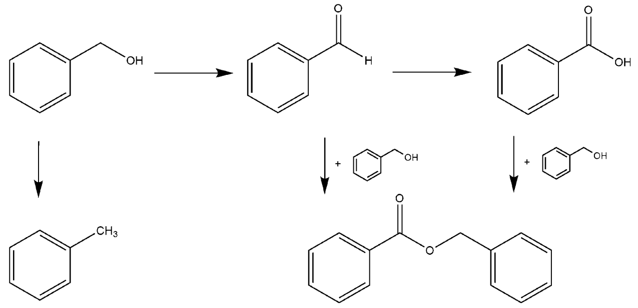

Scheme 1 Reaction pathway for the oxidation of benzyl alcohol.

Benzyl alcohol oxidation

The catalytic oxidation of benzyl alcohol was used to probe the activity, recovery and recyclability of the supported AuPd NP catalysts. The possible products of the oxidation of benzyl alcohol are summarized in Scheme 1.

The effects of reaction temperature and oxygen pressure were investigated, and the results obtained with the Fe_3O_4@SiO_2-NH_2–AuPd catalyst are shown in Table 2. Increasing the temperature from 60 to 100 °C showed a marked effect on the rate of the reaction, which changed from about 4% to 92% conversion, while only a minor effect on the selectivity to benzaldehyde was seen, decreasing from 100 to 90% with increasing temperature. Decreasing the oxygen pressure from 6 to 2 bar O_2 had a strong influence on the rate of the reaction, which dropped from 92 to 48% conversion, and consequently the selectivity towards benzaldehyde increased. In view of this, reactions were carried out at a temperature of 100 °C and 6 bar in order to increase conversion to the desired benzaldehyde product (Table 2, entry 3). The benzyl alcohol conversion curve and the product distribution over time are shown in Fig. 3. Benzaldehyde was the major product of benzyl alcohol oxidation with the AuPd NP catalyst, but after 80% conversion, the selectivity for benzaldehyde decreased with the formation of benzoic acid.

Table 2 Oxidation of benzyl alcohol by Fe_3O_4@SiO_2-NH_2–AuPd

				Selectivity[c] (%)			
Entry[a]	P O_2 (bar)	T (°C)	Conv.[b] (%)	I	II	III	IV
1	6	60	3.8	—	100	—	—
2	6	80	17.3	—	97.1	1.9	1.0
3	6	100	92.1	<1	90.1	7.2	1.3
4	4	100	82.5	<1	95.5	2.0	1.9
5	2	100	48.5	<1	96.8	1.8	1.0

[a] Reaction conditions: benzyl alcohol (9.6 mmol), 75 mg catalyst (4.3×10^{-3} mmol Au + Pd), 2.5 h. [b] Determined by GC. [c] I refers to toluene, II refers to benzaldehyde, III refers to benzoic acid and IV refers to benzyl benzoate.

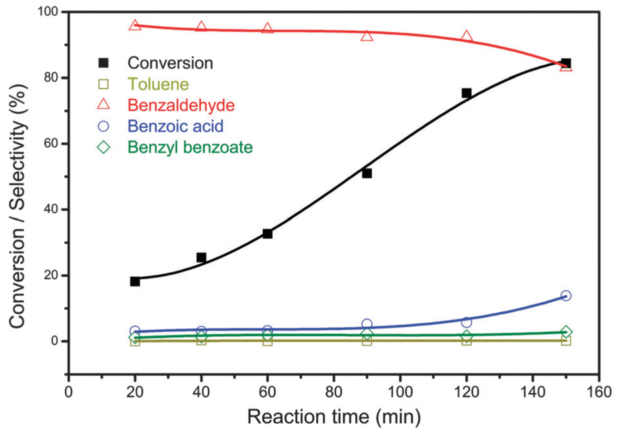

Fig. 3 Effect of the reaction time on the conversion and selectivity in the solvent-free oxidation of benzyl alcohol (at 100 °C and 6 bar O_2) over the Au–Pd magnetic catalyst.

Influence of the catalyst support

As mentioned before, functionalized supports improved the uptake of metal NPs from their colloidal solution (the coordination capture method) and allowed the preparation of catalysts loaded with three times more metal (Au + Pd) than the non-functionalized support. In principle, we realized that the functional groups grafted on the support surface allowed a more efficient adsorption of metal NPs, probably due to a stronger interaction of the AuPd NPs with the functionalized support than with the silanol groups of the non-functionalized support. At this point, we questioned if those functional groups grafted on the support could influence the catalytic properties of supported metal NPs. We decided to investigate how different ligands might affect the catalytic activity of supported AuPd NPs, again using benzyl alcohol oxidation to probe the activity, recovery and recyclability of the supported AuPd NP catalysts. We observed that the presence of functional groups had a major influence on the stability and reusability of the catalysts. The catalysts prepared with functionalized supports containing –NH_2 groups (Fe_3O_4@SiO_2-NH_2–AuPd) exhibited higher activity and stability towards catalyst recycling (Table 3, entries 1–5) than the functionalized support containing –SH groups (Fe_3O_4@SiO_2-SH–AuPd) and the non-functionalized catalyst. The catalyst prepared with the non-functionalized support Fe_3O_4@SiO_2–AuPd was less active (Table 3, entries 8 and 9) and exhibited metal leaching during recycling.

Table 3 Oxidation of benzyl alcohol by bimetallic AuPd supported on Fe_3O_4@SiO_2 with different functional groups

				Selectivity[c] (%)			
Entry[a]	Functional groups	Cycle	Conversion[b] (%)	I	II	III	IV
1	NH_2	1	62.7	<1	85.6	12.6	1.9
2	NH_2	2	49.3	<1	86.6	11.8	1.6
3	NH_2	3	41.4	<1	85.1	13.4	1.5
4	NH_2	4	28.4	<1	74.8	23.0	2.2
5	NH_2	5	33.8	<1	80.8	17.5	1.8
6	SH	1	73.6	5.8	69.8	22.1	2.3
7	SH	2	13.7	28.1	71.9	<1	<1
8	—	1	1.0	<1	70.7	29.2	<1
9	—	2	1.0	<1	44.5	55.5	<1

[a] Reaction conditions: benzyl alcohol (9.6 mmol), 75 mg catalyst, 2.5 h. [b] Determined by GC. [c] I refers to toluene, II refers to benzaldehyde, III refers to benzoic acid and IV refers to benzyl benzoate.

This journal is © The Royal Society of Chemistry 2013

Published on 19 July 2013. Downloaded by State University of New York at Stony Brook on 30/10/2014 15:17:32.

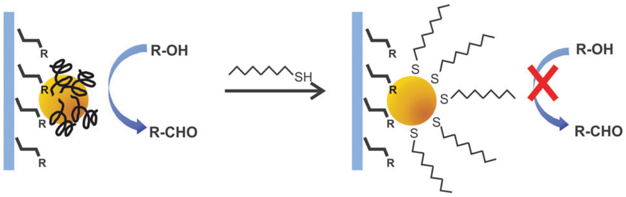

Fig. 4 Schematic representation of stabilizer exchange by the addition of 1-octanethiol.

Moreover, differences in the catalytic behavior of Fe_3O_4@SiO_2-SH–AuPd and Fe_3O_4@SiO_2-NH_2–AuPd were noted in the conversion of benzyl alcohol under similar reaction conditions. The Fe_3O_4@SiO_2-NH_2–AuPd catalyst exhibited 62.7% conversion of benzyl alcohol in the first reaction and then a steady decrease in activity in the subsequent recycles, although the selectivity was maintained (Table 3, entries 1–5). The Fe_3O_4@SiO_2-SH–AuPd catalyst exhibited 73.6% conversion of benzyl alcohol in the first reaction, then a sudden decrease in activity in the subsequent reaction cycle (Table 3, entries 6 and 7). This catalyst with SH-groups formed more toluene than the others, which suggests the disproportionation of benzyl alcohol. The presence of thiol groups, known to poison gold catalyst surfaces, may have been responsible for blocking the activity of supported AuPd NPs upon recycling. A similar effect was obtained by the addition of 5 equiv. of 1-octanethiol to our catalyst during the oxidation of benzyl alcohol, which irreversibly reduced the catalytic activity (Fig. 4).

Major differences were observed in the product distribution when comparing Fe_3O_4@SiO_2-NH_2–AuPd and Fe_3O_4@SiO_2-SH–AuPd: (i) benzaldehyde was the main product, but a higher selectivity of 85.6% was achieved with the amino-functionalized catalyst compared to the thiol-functionalized catalyst (69.8%); (ii) benzoic acid was formed by both catalysts, but this product was formed in larger amounts by the thiol-functionalized catalyst (22%) than by the amino-functionalized catalyst (12.6%); (iii) toluene formation was negligible with the amino-functionalized catalyst, but reached 6% to 28% with the thiol-functionalized catalyst. All these observations regarding conversion and selectivity suggest that the amino-functionalized catalyst is more selective for the desired benzaldehyde product and produces fewer unwanted by-products, for example toluene. However, the decrease in activity in successive reaction cycles revealed the need for further studies on this system. It is worth mentioning that catalyst recovery by placing a permanent magnet in the reactor wall was slower and less efficient for the Fe_3O_4@SiO_2-NH_2–AuPd catalyst after the first reaction than for Fe_3O_4@SiO_2-SH–AuPd, indicating changes at the material surface that make it more stable in solution after the reaction. A plausible reaction that can take place on Fe_3O_4@SiO_2-NH_2–AuPd, but not Fe_3O_4@SiO_2-SH–AuPd, is the formation of an aldimine by the reaction of NH_2 groups grafted onto the catalyst support with the benzaldehyde formed during the oxidation of benzyl alcohol. Unfortunately, we could not follow the formation of –C═N bonds by FT-IR because Fe_3O_4@SiO_2 contains broad and strong vibrational bands of Si–OH, Si–O, and Si–O–Si typical of amorphous silica that overlay the features corresponding to ν(C═N) at ~1630 cm^{-1}. We also tried to follow the strong absorption expected for imine groups at ~400 cm^{-1} by UV-Vis spectrometry, but again the observation in hindered by the absorption of the Fe_3O_4@SiO_2 support. A set of experiments using silica (without iron oxide on it) clearly showed that amino-functionalized silica reacts with benzaldehyde to give a yellow solid with a strong UV-Vis absorption at 400 cm^{-1}, confirming the hypothesis of a reaction of free amino groups with the reaction product (benzaldehyde) is plausible. In order to reinforce the presence of amino groups as the main reason for stabilization and difficult separation of the catalysts after the reaction, these groups were removed by calcination. Elemental CHN analysis of the pristine Fe_3O_4@SiO_2-NH_2–AuPd catalyst (0.34 %N, 2.85 %C, 1.53 %H) and of the calcined Fe_3O_4@SiO_2-NH_2–AuPd(C) catalyst (0.34 %N, 2.85 %C, 1.53 %H) revealed a marked decrease in the organic portion of the catalyst upon calcination, which suggests that most of the amino groups were removed. Consequently, the metal content determined by FAAS (Au = 0.78 wt% and Pd = 0.37 wt%) increased to 0.074 mmol (Au + Pd) g^{-1}, but the 1 : 1 Au : Pd molar ratio was maintained.

The calcined Fe_3O_4@SiO_2-NH_2–AuPd(C) catalyst was used in the oxidation of benzyl alcohol under similar conditions. The results are summarized in Table 4, together with the catalytic results for Fe_3O_4@SiO_2–AuPd(C) and Fe_3O_4@SiO_2-SH–AuPd(C) after calcination. The first important observation is that, after the removal of –NH_2 groups, the catalyst does not react with the reaction product benzaldehyde, as before, which resulted in fast and highly efficient catalyst recovery. Moreover, the calcined catalyst Fe_3O_4@SiO_2-NH_2–AuPd(C) was highly active and selective (88% benzaldehyde at 85% conversion), and was recyclable for up to five successive reactions without deactivation or changes in selectivity (Table 4, entries 1–5). The Fe_3O_4@SiO_2-SH–AuPd(C) catalyst was also highly active but was deactivated in the second reaction (Table 4, entries 6 and 7), while the Fe_3O_4@SiO_2–AuPd(C) catalyst did not show any activity after calcination (Table 4, entries 8 and 9).

Table 4 Oxidation of benzyl alcohol by bimetallic AuPd supported catalysts after calcination

				Selectivity[c] (%)			
Entry[a]	Catalyst	Cycle	Conversion[b] (%)	I	II	III	IV
1	d	1	85.3	<1	88.4	8.3	2.6
2	d	2	73.5	1.0	92.6	3.9	2.5
3	d	3	72.1	<1	94.9	1.6	2.9
4	d	4	59.2	2.5	91.0	3.7	2.8
5	d	5	80.4	<1	92.6	3.9	2.8
6	e	1	86.7	1.2	77.8	16.3	4.7
7	e	2	39.6	3.0	91.6	2.9	2.5
8	f	1	2.5	<1	19.0	81.0	<1
9	f	2	3.6	<1	7.3	92.7	<1

[a] Reaction conditions: benzyl alcohol (9.6 mmol), 75 mg catalyst, 2.5 h. [b] Determined by GC. [c] I refers to toluene, II refers to benzaldehyde, III refers to benzoic acid and IV refers to benzyl benzoate. [d] Fe_3O_4@SiO_2-NH_2–AuPd(C). [e] Fe_3O_4@SiO_2-SH–AuPd(C). [f] Fe_3O_4@SiO_2–AuPd(C).

Published on 19 July 2013. Downloaded by State University of New York at Stony Brook on 30/10/2014 15:17:32.

We anticipated that thermal treatment would not change the magnetic response of the support, which was magnetically recovered before and after calcination using the same permanent magnet. The size and size distribution of the bimetallic AuPd NPs in the calcined catalyst before use, $Fe_3O_4@SiO_2$-NH_2–AuPd(C), and the calcined catalyst after five reuses in successive oxidations of benzyl alcohol, $Fe_3O_4@SiO_2$-NH_2–AuPd(C)-R5 were assessed by the analysis of TEM micrographs (Fig. S2 and S3, ESI†). The core–shell nanostructure of the catalyst support $Fe_3O_4@SiO_2$ was maintained after calcination and the mean size of the AuPd NPs increased from 5.1 ± 1.2 nm (before calcination – Fig. S1, ESI†) to 6.8 nm (σ = 0.38) (after calcination – Fig. S2, ESI†) and to 9.3 nm (σ = 0.45) (after five reuses – Fig. S3, ESI†). Additionally, the recycled catalyst showed signs of support agglomeration and the AuPd NPs grew at a moderate rate when compared with the monometallic Au NPs reported previously.[11]

Possible changes in the catalysts after thermal treatment and after recycling were investigated by X-ray photoelectron spectroscopy (XPS). The Pd(3d)/Au(4d) XPS spectra for the pristine $Fe_3O_4@SiO_2$-NH_2–AuPd catalyst, the calcined $Fe_3O_4@SiO_2$-NH_2–AuPd(C) catalyst before use and the calcined catalyst after five reuses in successive oxidations of benzyl alcohol, $Fe_3O_4@SiO_2$-NH_2–AuPd(C)-R5, are shown in Fig. 5. Analysis of the Pd(3d5/2) spectra was complicated by the overlap of the Pd(3d5/2) doublet and the Au(4d5/2) component. However, deconvolution of the XPS spectra revealed the contribution of each metal. The Pd(3d5/2) and the Au(4d5/2) peaks of the calcined $Fe_3O_4@SiO_2$-NH_2–AuPd(C) catalyst (Fig. 5B) exhibit a significant chemical shift to higher binding energies when compared with the uncalcined catalyst (Fig. 5A); this can be attributed to the oxidation of Au and Pd species upon calcination. However, after the calcined catalyst was reused in five successive reactions, the XPS peaks shifted back to lower binding energies, suggesting the reduction of Au and Pd species (Fig. 5C). Another important feature in the XPS spectra in Fig. 5A and B is the enrichment of Pd on the surface of the AuPd NPs. The Pd/Au molar ratio increased from 0.72 to 1.78 after calcination. Additionally, the Pd/Au molar ratio of the reused catalyst was maintained at 1.58 (Fig. 5C). The XPS results indicate that Pd surface segregation occurs during calcination, producing a Pd-rich shell on the AuPd NPs, which is in agreement with the literature,[27] and the catalyst retained the Pd surface enrichment upon recycling. The XPS analysis and the catalyst recycling results corroborate the high stability of the catalyst upon recycling.

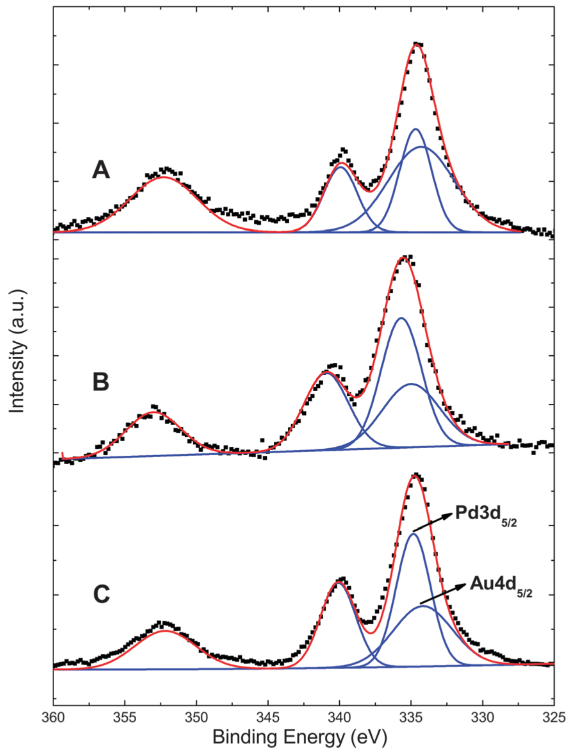

Fig. 5 Au(4d) and Pd(3d) X-ray photoelectron spectra of the $Fe_3O_4@SiO_2$-NH_2–AuPd catalyst after different heat treatments: (A) uncalcined, (B) calcined at 500 °C and (C) the calcined catalyst after five reuses in successive oxidations of benzyl alcohol.

As far as we know, this is the first magnetically recoverable AuPd NP catalyst reported, even though other examples of catalysts for the selective oxidation of alcohols that are also magnetically retrievable can be found in the literature, for example those based on monometallic AuNPs.[11,24,28,29] The main advantage of AuPd catalysts is their high catalytic activity and selectivity in the absence of a base, which increases the catalyst's life span.

Conclusions

Pre-synthesized AuPd NPs stabilized by polyvinyl alcohol (PVA) were used as precursors to prepare well-defined catalysts, and silica-coated magnetite was used as a magnetically recoverable support. The main issue regarding the preparation of magnetically recoverable metal nanoparticle is obtaining a strong metal–support interaction to avoid nanoparticles coalescence, segregation and metal leaching during liquid phase reactions, while maintaining the catalytic properties of the selected nanoparticles. In order to attach the NPs to the support and improve metal–support interactions, we used a coordination capture method based on the functionalization of the support surface with ligands, such as amino and thiol groups, to provide coordination sites and keep the nanoparticles attached to the support. However, the ligands grafted onto the support surface affected the catalytic activity and selectivity of the supported AuPd NPs. Additionally, the amino groups provided stabilization in solution, but made it difficult to separate the catalyst after the reaction. We then demonstrated that catalytic activity and catalyst stability towards recycling could be improved upon removal of the functional groups by thermal treatment.

Acknowledgements

The authors are grateful to the Brazilian agencies FAPESP and CNPq for financial support and indebted to the Brazilian

This journal is © The Royal Society of Chemistry 2013

Published on 19 July 2013. Downloaded by State University of New York at Stony Brook on 30/10/2014 15:17:32.

Nanotechnology National Laboratory (LNNano, Campinas, Brazil) for HRTEM images and EDS analysis. The authors also acknowledge the Instituto Nacional de Ciência e Tecnologia de Catálise em Sistemas Moleculares e Nanoestruturados (INCT-CMN).

Notes and references

1 R. A. Sheldon and J. K. Kochi, *Metal-catalyzed oxidations of organic compounds: mechanistic principles and synthetic methodology including biochemical processes*, Academic Press, New York, 1981.

2 G. J. ten Brink, I. W. C. E. Arends and R. A. Sheldon, *Science*, 2000, **287**, 1636–1639.

3 C. P. Vinod, K. Wilson and A. F. Lee, *J. Chem. Technol. Biotechnol.*, 2011, **86**, 161–171.

4 A. S. K. Hashmi and G. J. Hutchings, *Angew. Chem., Int. Ed.*, 2006, **45**, 7896–7936.

5 A. S. K. Hashmi, C. Lothschütz, M. Ackermann, R. Doepp, S. Anantharaman, B. Marchetti, H. Bertagnolli and F. Rominger, *Chem.–Eur. J.*, 2010, **16**, 8012–8019.

6 F. Porta, L. Prati, M. Rossi, S. Coluccia and G. Martra, *Catal. Today*, 2000, **61**, 165–172.

7 L. Prati and G. Martra, *Gold Bull.*, 1999, **32**, 96–101.

8 L. Prati and M. Rossi, *J. Catal.*, 1998, **176**, 552–560.

9 S. Carrettin, P. McMorn, P. Johnston, K. Griffin, C. J. Kiely and G. J. Hutchings, *Phys. Chem. Chem. Phys.*, 2003, **5**, 1329–1336.

10 S. Biella, L. Prati and M. Rossi, *Inorg. Chim. Acta*, 2003, **349**, 253–257.

11 R. L. Oliveira, P. K. Kiyohara and L. M. Rossi, *Green Chem.*, 2010, **12**, 144–149.

12 N. Herron, S. Schwarz and J. D. Druliner, *WO Pat.*, 16298-A1, 2002.

13 D. I. Enache, J. K. Edwards, P. Landon, B. Solsona-Espriu, A. F. Carley, A. A. Herzing, M. Watanabe, C. J. Kiely, D. W. Knight and G. J. Hutchings, *Science*, 2006, **311**, 362–365.

14 P. Miedziak, M. Sankar, N. Dimitratos, J. A. Lopez-Sanchez, A. F. Carley, D. W. Knight, S. H. Taylor, C. J. Kiely and G. J. Hutchings, *Catal. Today*, 2011, **164**, 315–319.

15 P. J. Miedziak, Q. He, J. K. Edwards, S. H. Taylor, D. W. Knight, B. Tarbit, C. J. Kiely and G. J. Hutchings, *Catal. Today*, 2011, **163**, 47–54.

16 H. Zhang, Y. Xie, Z. Sun, R. Tao, C. Huang, Y. Zhao and Z. Liu, *Langmuir*, 2010, **27**, 1152–1157.

17 K. Kaizuka, H. Miyamura and S. Kobayashi, *J. Am. Chem. Soc.*, 2010, **132**, 15096–15098.

18 C.-J. Jia and F. Schueth, *Phys. Chem. Chem. Phys.*, 2011, **13**, 2457–2487.

19 F. Osterloh, H. Hiramatsu, R. Porter and T. Guo, *Langmuir*, 2004, **20**, 5553–5558.

20 O. P. Khatri, K. Adachi, K. Murase, K.-i. Okazaki, T. Torimoto, N. Tanaka, S. Kuwabata and H. Sugimura, *Langmuir*, 2008, **24**, 7785–7792.

21 M. J. Jacinto, P. K. Kiyohara, S. H. Masunaga, R. F. Jardim and L. M. Rossi, *Appl. Catal., A*, 2008, **338**, 52–57.

22 J. A. Lopez-Sanchez, N. Dimitratos, P. Miedziak, E. Ntainjua, J. K. Edwards, D. Morgan, A. F. Carley, R. Tiruvalam, C. J. Kiely and G. J. Hutchings, *Phys. Chem. Chem. Phys.*, 2008, **10**, 1921–1930.

23 J. H. Scofield, *J. Electron Spectrosc. Relat. Phenom.*, 1976, **8**, 129–137.

24 R. L. Oliveira, D. Zanchet, P. K. Kiyohara and L. M. Rossi, *Chem.–Eur. J.*, 2011, **17**, 4626–4631.

25 L. M. Rossi, I. M. Nangoi and N. l. J. S. Costa, *Inorg. Chem.*, 2009, **48**, 4640–4642.

26 N. Dimitratos, J. A. Lopez-Sanchez, J. M. Anthonykutty, G. Brett, A. F. Carley, R. C. Tiruvalam, A. A. Herzing, C. J. Kiely, D. W. Knight and G. J. Hutchings, *Phys. Chem. Chem. Phys.*, 2009, **11**, 4952–4961.

27 A. A. Herzing, A. F. Carley, J. K. Edwards, G. J. Hutchings and C. J. Kiely, *Chem. Mater.*, 2008, **20**, 1492–1501.

28 F. Mi, X. Chen, Y. Ma, S. Yin, F. Yuan and H. Zhang, *Chem. Commun.*, 2011, **47**, 12804–12806.

29 H. W. Chen, A. Murugadoss, T. S. A. Hor and H. Sakurai, *Molecules*, 2010, **16**, 149–161.